Elastic properties of amorphous boron suboxide based solids studied using *ab initio* molecular dynamics

2008 J. Phys.: Condens. Matter 20 195203

(http://iopscience.iop.org/0953-8984/20/19/195203)

IOP PUBLISHING JOURNAL OF PHYSICS: CONDENSED MATTER

J. Phys.: Condens. Matter **20** (2008) 195203 (5pp) doi:10.1088/0953-8984/20/19/195203

Elastic properties of amorphous boron suboxide based solids studied using *ab initio* molecular dynamics

Denis Music[1] **and Jochen M Schneider**

Materials Chemistry, RWTH Aachen University, Kopernikusstraße 16, D-52074 Aachen, Germany

E-mail: music@mch.rwth-aachen.de

Received 11 December 2007, in final form 22 February 2008
Published 8 April 2008
Online at stacks.iop.org/JPhysCM/20/195203

Abstract

We have studied the correlation between chemical composition, structure, chemical bonding and elastic properties of amorphous B_6O based solids using *ab initio* molecular dynamics. These solids are of different chemical compositions, but the elasticity data appear to be a function of density. This is in agreement with previous experimental observations. As the density increases from 1.64 to 2.38 g cm^{-3}, the elastic modulus increases from 74 to 253 GPa. This may be understood by analyzing the cohesive energy and the chemical bonding of these compounds. The cohesive energy decreases from −7.051 to −7.584 eV/atom in the elastic modulus range studied. On the basis of the electron density distributions, Mulliken analysis and radial distribution functions, icosahedral bonding is the dominating bonding type. C and N promote cross-linking of icosahedra and thus increase the density, while H hinders the cross-linking by forming OH groups. The presence of icosahedral bonding is independent of the density.

(Some figures in this article are in colour only in the electronic version)

1. Introduction

Boron suboxide (B_6O, space group $R\bar{3}m$) is a boron rich solid composed of icosahedra (B_{12} units) located at the nodes of a rhombohedral Bravais lattice, giving rise to unusual bonding [1, 2]. Each boron atom within an icosahedron has a coordination number $\geqslant 5$. Since the valence shell configuration is $2s^2 2p^1$, boron forms electron-deficient bonds with the highest electron density between three adjacent atoms within the icosahedron [3, 4]. B_6O is a semiconductor with the band gap of 2.4 eV [5] and exhibits a large melting point of 1760 °C [6]. Boron rich solids are characterized by a range of unusual properties, such as extraordinary radiation tolerance and large Seebeck coefficient [7]. Furthermore, B_6O possesses the bulk and elastic modulus of 230 and 476 GPa, respectively [8]. It is well known that the elastic properties are a function of density [9–12]. This has been observed for both crystalline B_6O bulk [8] and amorphous B_6O based thin films [13–15]. It is surprising that relatively large variations in the chemical composition for these amorphous thin films (O, C, N, H and Ar contents in the range up to 14.9, 0.6, 0.5 and 4.7 at.%, respectively) result in a similar elastic modulus–density dependence [13–15]. It appears that the elastic properties are controlled by the density and that they are only indirectly affected by chemical composition. However, this phenomenon is not understood.

In this work, the effect of the chemical composition on the elastic properties of amorphous B_6O based solids is studied by means of *ab initio* molecular dynamics (MD). The calculated elastic modulus data appear independent of the chemical composition, but are controlled by the density. This may be understood by analyzing the cohesive energy and the chemical bonding of these configurations. As the cohesive energy decreases, the elastic modulus increases. The dominating bonding type is icosahedral bonding throughout the density range probed. We suggest that it is possible to establish this elastic modulus–density dependence due to the existence of icosahedral bonding.

[1] Author to whom any correspondence should be addressed.

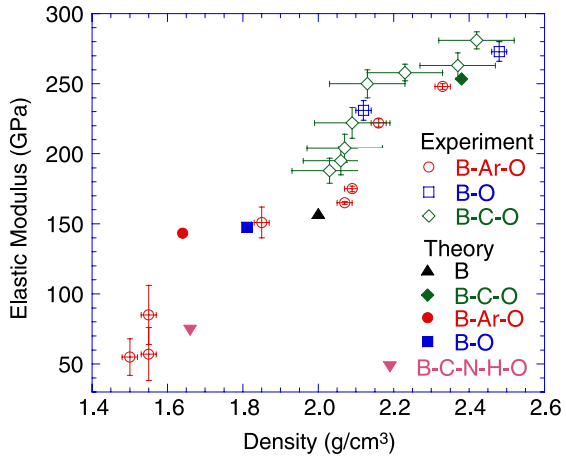

Figure 1. Elastic modulus as a function of density for amorphous B_6O based configurations, obtained by *ab initio* MD studies. Comparison is made with experimental data.

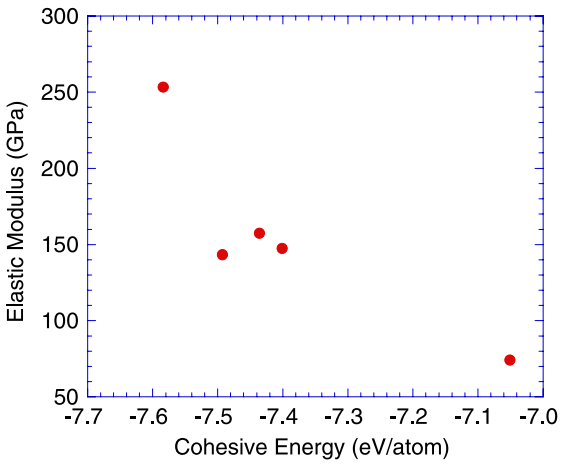

Figure 2. Elastic modulus as a function of cohesive energy for amorphous B_6O based configurations.

2. Computational details

The *ab initio* MD study was performed using the OpenMX code [16, 17], based on density functional theory [18] and basis functions in the form of linear combinations of localized pseudoatomic orbitals [19]. The electronic potentials were fully relativistic pseudopotentials with partial core corrections [20, 21] and the generalized gradient approximation was applied [22]. The basis functions used were generated by a confinement scheme [19, 23] and specified as follows: B4.5-s2p2, O4.5-s2p1, Ar5.0-s2p1, C4.5-s2p1, N4.5-s2p1 and H4.5-s2. The first symbol designates the chemical name, followed by the cutoff radius (in Bohr radius) in the confinement scheme and the last set of symbols defines the primitive orbitals applied. The energy cutoff (150 Ryd) and k-point grid ($1 \times 1 \times 1$) within the real space grid technique [24] were adjusted to reach the accuracy of 10^{-6} H/atom. An electronic temperature of 700 K is used to count the number of electrons using the Fermi–Dirac distribution function. In all simulations, the MD time step was 1.0 fs. To create amorphous configurations, 96–156 atoms, with the positions taken from the α-B structure (space group $R\bar{3}m$), were run in a cubic supercell at the temperature of 3000 K within a canonical ensemble for 400 fs, by scaling the velocities. These configurations were then quenched to 0 K and relaxed for an additional 400 fs. Additional elements were inserted by substituting B atoms in the α-B structure and following the same procedure for the amorphous supercell construction. This procedure allows for creation of representative amorphous configurations [25]. The following configurations were considered (balance B): (i) B, (ii) B–O (2.1 at.% O), (iii) B–Ar–O (6.3 at.% Ar, 2.1 at.% O), (iv) B–C–O (1.0 at.% C, 2.1 at.% O) and (v) B–C–N–H–O (2.1 at.% C, 1.0 at.% N, 10.4 at.% H, 20.8 at.% O). These configurations were chosen on the basis of the experimentally determined chemical composition [13–15, 26]. The bulk modulus was calculated from the pressure–volume data and assuming the Poisson's ratio of 0.2, as in nanoindentation experiments [13–15, 26], and an isotropic medium, the elastic modulus was calculated. The density was calculated from the energy–volume data. The cohesive energy was obtained by subtracting the total energy of each configuration at 0 K from the total energy of isolated atoms. The electronic structure was studied using Mulliken populations [27], electron density distributions and radial distribution functions (RDF).

3. Results and discussion

The analysis of *ab initio* MD data is started by evaluating the elastic modulus values obtained. In figure 1, the calculated elastic modulus data are given as a function of the calculated density. As the density increases from 1.64 to 2.38 g cm^{-3}, by a factor of 1.5, the elastic modulus increases from 74 to 253 GPa, by a factor of 3.4. These data are consistent with experimental values [13–15], with the exception of the B–Ar–O configuration. This may be due to the fact that the experimentally analyzed samples contain Ar bubbles [13], ranging up to 10 nm in diameter, while this is not the case for the MD configuration. The experimentally observed microstructure cannot be simulated with the configuration size used, since more than 1000 atoms are required, which is computationally too demanding for *ab initio* MD studies. Nevertheless, it is clear that the elastic modulus exhibits a linear relationship with the density in the range studied. The most striking feature is that these configurations are of different chemical compositions, as described above, but the elasticity data appear to be a function of density.

In order to shed more light on this relationship, we analyze the cohesive energy of the configurations obtained in this work. In figure 2, the elastic modulus data are plotted as a function of the cohesive energy values. As the cohesive energy decreases from −7.051 to −7.584 eV/atom, the elastic modulus increases from 74 to 253 GPa. This is a smooth function, again with an exception of the B–Ar–O configuration, as already discussed above. The cohesive energies obtained are consistent with those for the bulk B_6O and B_4C [28]. This elastic modulus–cohesive energy dependence is also consistent with experimental and theoretical data for the

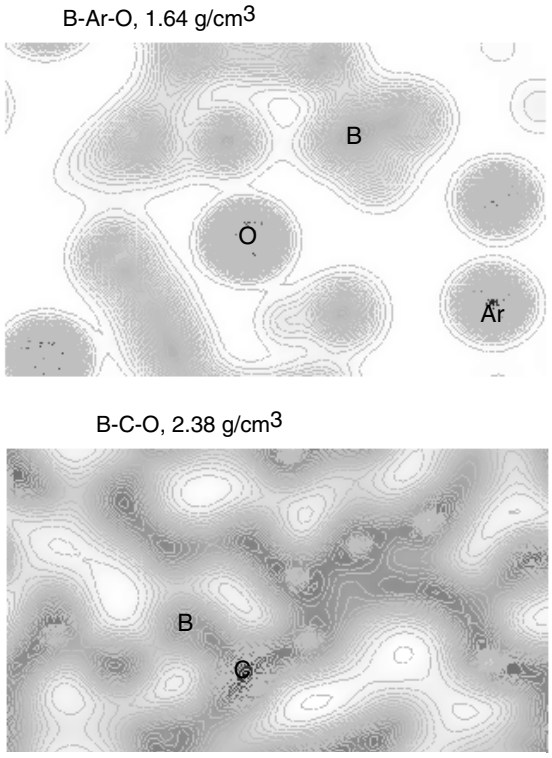

Figure 3. Electron density distribution in the (110) plane for amorphous B_6O based configurations with densities of 1.64 and 2.38 g cm^{-3}. The electron density distribution increases from 0.0 (white) to 0.4 (dark gray) electrons $Å^{-3}$.

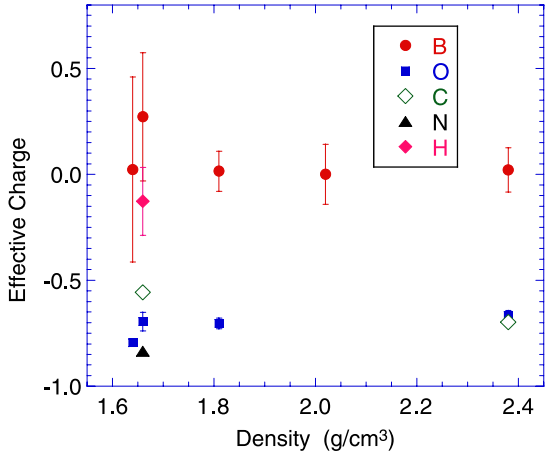

Figure 4. Effective charge in amorphous B_6O based configurations as a function of density.

Al–O–H system [9]. Since it is possible to correlate the elastic modulus and the cohesive energy of these B based configurations, this may indicate that a similar kind of chemical bonding is present.

To test this hypothesis, we study the chemical bonding in the configurations considered. In figure 3, the electron density distribution in the (110) plane is given for the B–Ar–O and B–C–O configurations, chosen to be representatives for the chemical bonding analysis. Some remarks can be made about these electron density distributions. Firstly, these configurations appear amorphous, since there is no long-range order in terms of the atomic positions. Secondly, B atoms share the charge, and cross-sections of spherically depleted regions are also visible. This is consistent with the icosahedral bonding [3, 4]. Analyzing the atomic structure of these configurations, we observe B_3 clusters (triangles) often merged into larger 3D networks resembling B_{12} units or parts thereof. Thirdly, B and O also share electrons, which is consistent with covalent bonding, and due to electronegativity differences, some charge transfer can be expected. Fourthly, Ar is not contributing to the bonding. To provide more details on the chemical bonding for all configurations explored, the effective charge is provided in figure 4 as a function of the density. Here, the effective charge is referring to a difference between the charge of a neutral atom and the total charge that it possesses in a compound [29]. The average effective charge for B is +0.07, independently of the density. It is worth noting that the B effective charge exhibits the largest spread. This is consistent with icosahedral bonding, since the B effective charge in crystalline B_6O ranges from −0.05 to +0.20 [5]. This spread is due to the smaller difference in bonding between polar and equatorial B atoms in icosahedrally bonded solids [30]. The average effective charge for O is −0.71, again independently of the density. This is also consistent with the icosahedral bonding in crystalline B_6O, where the effective charge for O is −0.51 [5]. Furthermore, this independence of density is consistent with our previous work where we showed, using classical MD, that the B–B and B–O bond lengths are not a function of the O content and hence density [14]. The average effective charges for C and N are −0.63 and −0.84, respectively. The role of C and N in crystalline icosahedrally bonded solids is to cross-link icosahedra and they exhibit the effective charges of −0.64 and −0.53, respectively [30]. Hence, C and N may cross-link icosahedra (or parts thereof) in these amorphous configurations. In amorphous B–C films, C was reported to hinder the formation of the continuous network of B_{12} units, but shortens the bond length as is expected in icosahedrally bonded B_4C [31]. This is consistent with our previous work on amorphous B–C–O films where the increase in the C content was correlated with the increase in the density and the elastic modulus [15], which in turn may indicate that the bonding nature is not a function of the chemical composition. The average effective charge for H is −0.13. It is well known that B rich compounds form $H_3(BO)_3$ upon exposure to air [32–34]. Together with negatively changed O, H forms OH groups as is expected in the $H_3(BO)_3$ structure and its effective charge is consistent with previous work on various hydroxide complexes [35]. The formation of OH groups may disrupt the cross-linking of icosahedra. Another bonding type found in these configurations was the B–H bond, which is also consistent with the H effective charge [36]. The B–H bonding may also be present in icosahedrally bonded solids [37], but it may also disrupt the strong cross-linking of icosahedra. To conclude at this point, these average effective changes imply that the typical bonding in these configurations is of icosahedral nature and that there are no significant changes in the effective charge, and hence the nature of chemical bonding, as a function of density.

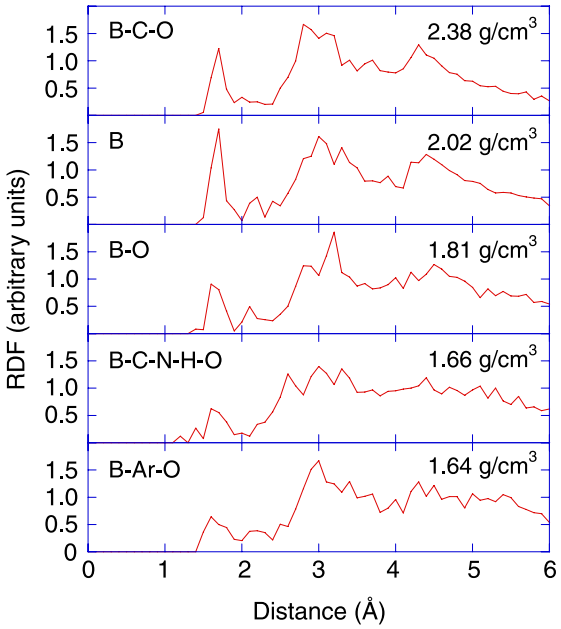

Figure 5. Radial distribution functions (RDF) of amorphous B_6O based configurations for all densities studied.

After analyzing the chemical bonding in these amorphous B_6O based configurations, it is important to determine the relevance of the bonding types found. In figure 5, RDF data are given for all configurations. Firstly, these RDF curves are continuous, which is indicative of amorphous structure. They are consistent with previous work [14, 38]. Secondly, the dominating peak is at approximately 1.7 Å, independently of the density. This is consistent with icosahedral bonding, since in crystalline α-B, B_4C, B_6N, B_6O, B_6P and B_6As, the icosahedral bond length is in the range from 1.68 to 1.75 Å [30]. This is also consistent with x-ray photoelectron spectroscopy data on amorphous B_6O based solids [39]. RDF data may be used to discuss extreme density variations, as shown for B–C–O and B–C–N–H–O configurations. In both cases, the most dominating bonding type is icosahedral, but there are some subtle differences. The icosahedral peak for B–C–O is larger than that for B–C–N–H–O, while there are even shorter bonds in B–C–N–H–O. However, these shorter bonds may be attributed to OH and B–H, as discussed above, which both disrupt the cross-linking of icosahedra. Other reasons for the density differences may be found in clustering between icosahedra or fragments thereof. Even though icosahedra may be effectively cross-linked, like in the case of the B–C–O configuration, they may not cluster to form high density structures.

In many network-forming glasses, glass-forming ability is usually associated with the existence of three-dimensional random networks [40]. For instance, in B_2O_3 glasses boroxol rings and BO_3 triangles are present [40]. Hence, our B_6O based amorphous structures resemble these glasses due to the icosahedral networks found. Furthermore, low temperature anomalies, for instance in heat capacity, may occur in glasses and can be related to the vibrational dynamics, the so-called 'boson peak', since there is an excess of the low energy density of states in glasses relative to the Debye model [41]. This boson peak may be related to the elastic inhomogeneities at low scales, e.g. <33 Å in SiO_2 glass [41]. In our case, differences in vibrational dynamics between crystalline B_6O and B_6O based amorphous configurations with extreme density variations may be expected, as shown for B–C–O and B–C–N–H–O.

4. Conclusions

We have studied the correlation between chemical composition, structure, chemical bonding and elastic properties of amorphous B_6O based solids using *ab initio* MD. These configurations are of different chemical compositions, but the elasticity data appear to be a function of density. This is consistent with experimental data [13–15]. As the density increases from 1.64 to 2.38 g cm^{-3}, by a factor of 1.5, the elastic modulus increases from 74 to 253 GPa, by a factor of 3.4. This may be understood by analyzing the cohesive energy and the chemical bonding of these configurations. The cohesive energy decreases from −7.051 to −7.584 eV/atom in the elastic modulus range studied. On the basis of the investigation of the electronic structure thereof, icosahedral bonding is the dominating bonding type. C and N promote cross-linking of icosahedra and thus increase the density, while H hinders the cross-linking by forming OH groups. The presence of icosahedral bonding is not affected by the density.

Acknowledgment

This study was financially supported by DFG (Schn 735/12-1, 'Mechanical properties of YM_3B phases').

References

[1] Hubert H, Devourd B, Garvie L A J, O'Keeffe M, Busseck P R, Petuskey W T and McMillan P F 1998 *Nature* **391** 376
[2] Emin D 1987 *Phys. Today* **40** 55
[3] Longuet-Higgins H C and Roberts M de V 1955 *Proc. R. Soc.* A **230** 110
[4] Music D and Schneider J M 2005 *Scr. Mater.* **52** 29
[5] Li D and Ching W Y 1996 *Phys. Rev.* B **54** 1451
[6] McMillan P F, Hubert H, Chizmeshya A, Petuskey W T, Garvie L A J and Devouard B 1999 *J. Solid State Chem.* **147** 281
[7] Emin D 2006 *J. Solid State Chem.* **179** 2791
[8] Petrak D R, Ruh R and Atkins G R 1974 *Ceram. Bull.* **53** 569
[9] Schneider J M, Larsson K, Lu J, Olsson E and Hjövarsson B 2002 *Appl. Phys. Lett.* **80** 1144
[10] Ma H-S, Roberts A P, Prévost J-H, Jullien R and Scherer G W 2000 *J. Non-Cryst. Solids* **277** 127
[11] El Khakani M A, Chaker M, O'Hern M E and Oliver W C 1997 *J. Appl. Phys.* **82** 4310
[12] Fan H, Hartshorn C, Buchheit T, Tallant D, Assink R, Simpson R, Kissel D J, Lacks D J, Torquato S and Brinker C J 2007 *Nat. Mater.* **6** 418
[13] Music D, Kreissig U, Czigány Z, Helmersson U and Schneider J M 2003 *Appl. Phys.* A **76** 269
[14] Music D, Kreissig U, Chirita V, Schneider J M and Helmersson U 2003 *J. Appl. Phys.* **93** 940

[15] Music D, Kugler V M, Czigány Z, Flink A, Werner O, Schneider J M, Hultman L and Helmersson U 2003 *J. Vac. Sci. Technol.* A **21** 1355
[16] Ozaki T and Kino H 2005 *Phys. Rev.* B **72** 045121
[17] OpenMX version 3.3 was used in this work and is available at www.openmx-square.org
[18] Hohenberg P and Kohn W 1964 *Phys. Rev.* **136** B864
[19] Ozaki T 2003 *Phys. Rev.* B **67** 155108
[20] Troullier N and Martins J L 1991 *Phys. Rev.* B **43** 1993
[21] Blöchl P E 1990 *Phys. Rev.* B **41** 5414
[22] Perdew J P, Burke K and Ernzerhof M 1996 *Phys. Rev. Lett.* **77** 3865
[23] Ozaki T and Kino H 2004 *Phys. Rev.* B **69** 195113
[24] Soler J M, Artacho E, Gale J D, Garcia A, Junquera J, Ordejon P and Sanchez-Portal D 2002 *J. Phys.: Condens. Matter* **14** 2745
[25] Zhang X and Drabold D A 1999 *Phys. Rev. Lett.* **83** 5042
[26] Music D, Kölpin H, Atiser A, Kreissig U, Bobek T, Hadam B and Schneider J M 2005 *Mater. Res. Bull.* **40** 1345
[27] Mulliken R S 1955 *J. Chem. Phys.* **23** 1833
[28] Lee S, Kim S W, Bylander D M and Kleinman L 1991 *Phys. Rev.* B **44** 3550
[29] Allred A L and Rochow E G 1958 *J. Inorg. Nucl. Chem.* **5** 264
[30] Guo X, He J, Liu Z, Tian Y, Sun J and Wang H-T 2006 *Phys. Rev.* B **73** 104115
[31] Shirai K, Emura S, Gonda S and Kumashiro Y 1995 *J. Appl. Phys.* **78** 3392
[32] Music D, Schneider J M, Kugler V, Nakao S, Jin P, Östblom M, Hultman L and Helmersson U 2002 *J. Vac. Sci. Technol.* A **20** 335
[33] Huang H, Ong C W, Zheng B, Kwok R W M, Lau W M and He J W 2003 *J. Vac. Sci. Technol.* A **21** 1595
[34] Erdemir A, Bindal C and Fenske G R 1996 *Appl. Phys. Lett.* **68** 1637
[35] Zhu M and Pan G 2005 *J. Phys. Chem.* A **109** 7648
[36] Zhang J, Zhang L, Cui T, Li Y, He Z, Ma Y and Zou G 2007 *Phys. Rev.* B **75** 104115
[37] Quong A A, Pederson M R and Broughton J Q 1994 *Phys. Rev.* B **50** 4787
[38] Kobayashi M, Higashi I and Takami M 1997 *J. Solid State Chem.* **133** 211
[39] Ong C W, Huang H, Zheng B, Kwok R W M, Hui Y Y and Lau W M 2004 *J. Appl. Phys.* **95** 3527
[40] Huang L and Kieffer J 2006 *Phys. Rev.* B **74** 224107
[41] Léonforte F, Tanguy A, Wittmer J P and Barrat J-L 2006 *Phys. Rev. Lett.* **97** 055501